Environmental Engineering and Management Journal October 2019, Vol. 18, No. 10, 2273-2285
http://www.eemj.icpm.tuiasi.ro/; http://www.eemj.eu

"Gheorghe Asachi" Technical University of Iasi, Romania

SMART WATER AND SOIL-SALINITY MANAGEMENT IN AGRO-WETLANDS

Marinella Masina[1*], Roberta Calone[2], Lorenzo Barbanti[2], Claudio Mazzotti[3], Alberto Lamberti[1], Maria Speranza[2]

[1]Alma Mater Studiorum Università di Bologna, Dipartimento di Ingegneria Civile, Chimica, Ambientale e dei Materiali - DICAM, viale del Risorgimento 2, 40136 Bologna, Italy
[2]Alma Mater Studiorum Università di Bologna, Dipartimento di Scienze e Tecnologie Agro-Alimentari - DISTAL, viale G. Fanin 44, 40127 Bologna, Italy
[3]Agrisfera S.Coop.Agr.p.a., via B. Nigrisoli 46, 48123 S. Alberto Ravenna, Italy

Abstract

Soil salinization is becoming worldwide one of the most serious land degradation issues. Seawater intrusion in upper aquifers is responsible for the largest proportion of salt-affected agricultural lands in coastal areas. In this study, the impact of different irrigation strategies on the salinity of a maize cultivated field located in the coastal plain of Ravenna, Italy, was simulated with the FAO AquaCrop model. Model calibration was supported by comparison with remote-sensed and field collected crop data. Ten irrigation scenarios were tested by varying the irrigation season length, the soil moisture threshold for irrigation (TI), and the irrigation depth (ID), in presence or absence of flooded pipe drains (FD) to create a fresh-water lens preventing salt rising from brackish groundwater.
FD show to be more effective in countering soil salinization than strategies exclusively based on supplying enough water to obtain salt leaching (SL). The best result, in terms of both fodder maize yield and salinization control, is achieved with the combination: FD immediately after sowing, irrigation inhibited in May, TI set at 50% of soil readily available water (RAW), and ID modulated to exceed field capacity and obtain SL. The worse strategy is revealed to be the non-FD scenario, coupled with no irrigation in May and August, TI ranging between 65 and 80% of soil RAW depletion, and ID set at 50 mm. Even if water-conservative, this approach results in high soil salinization and leads to significant yield decrease.

Key words: AquaCrop, groundwater, irrigation, maize, soil salinity

Received: August, 2019; Revised final: September, 2019; Accepted: October, 2019; Published in final edited form: October, 2019

1. Introduction

Salinization is the process by which water-soluble salts accumulate in soils. It is a concern because salt excess diminishes crop yields by limiting root water uptake and causes de-flocculation of clay particles decreasing soil porosity, which, in turn, reduces soil permeability, hydraulic conductivity (Crescimanno et al., 1995; Shainberg et al., 1992; Tsanis et al., 2016) and capacity to support equipment. Salts may be present in the soil since its formation or accumulated by water transport and evaporation. Tóth et al., (2008) show that salinization in Europe is a diffused problem along coastlines, particularly in the semiarid Mediterranean area. Seawater intrusion in river outlets and contamination of shallow coastal aquifers is actually also a worldwide growing issue due to sea level rise and land subsidence and, depending on site-specific topography and geomorphology, the presence of a saline groundwater determines a more or less intense soil salinization threatening coastal ecosystems. The process is

* Author to whom all correspondence should be addressed: e-mail: marinella.masina2@unibo.it.

jeopardizing soil integrity, water quality, vegetation biodiversity, and agricultural productivity of these habitats in the Mediterranean basin.

The Ravenna coastline in the Emilia-Romagna region, Italy, bordered northwards by Comacchio lagoon and southwards by Cervia town, is an area increasingly prone to the occurrence of the mentioned processes. A natural subsidence (up to 1.5 mm/year), due to the compaction of the alluvial deposits, has dropped this territory below the sea-level, requiring the establishment of an artificial drainage system. An extensive hydraulic infrastructure, composed by ditches, canals and pumps, was built between 1920 and 1960 to keep the land dry by continuously extracting soil water. The drainage, however, lowered the hydraulic head below the sea level and generated a hydraulic gradient promoting seawater inflow into the groundwater. In addition, the intense urbanization occurring in this area between 1950 and 1980, combined with water and methane extraction from the subsoil and phreatic aquifer exploitation for agriculture, have heavily intensified the subsidence rate (Teatini et al., 2006). The consequent saline seepage led to an average rising of the never stable freshwater–saltwater interface towards the ground surface in the low part of the area determining a more or less intense soil salinization (Antonellini et al., 2008; Buscaroli and Zannoni, 2010; Felisa et al., 2013; Greggio et al., 2012).

The measures currently applied to reclaim salt-affected sites are categorized into physical, chemical, biological, and hydraulic ones. This last, based on salt leaching (SL) through irrigation, is considered the main salinity control method in irrigated lands (Abrol et al., 1988; Visconti et al., 2011). During the growing season, SL can be accomplished by applying an amount of water exceeding soil water holding capacity. The additional water percolates downwards, moving salts below the root zone. A subsurface draining network is then required to collect and discharge the drained saline water.

To determine time and amount of water at each SL intervention, several factors must be considered, including: irrigation method and water quality, soil physico-chemical and hydraulic properties, initial and final desired level of soil salinity, plant transpiration requirements and crop tolerance to salinity. As water for irrigation becomes increasingly scarce and agriculture is called to make a more environmentally and economically sustainable use of it, an accurate irrigation scheduling is necessary.

The project LIFE AGROWETLANDS II (LIFE15 ENV/IT/000423), in whose framework this work has been conducted, is intended to counteract soil salinization affecting the coastal farmlands through a targeted and efficient management of the water resources. To this aim, the crop water productivity model AquaCrop (Steduto et al., 2009) has been chosen as instrument for irrigation management, due to its relative simplicity coupled with the possibility of dealing with soil and water salinity.

In comparison with other crop yield models as DSSAT (Jones et al., 2003), CropSyst (Stöckle et al., 2003), APSIM (Keating et al., 2003), Hybrid-Maize (Yang et al., 2004), which require a large number of input parameters and detailed information about crop development, AquaCrop needs a relatively small number of explicit parameters (Vanuytrecht et al., 2014), which can be easily obtained. Moreover, AquaCrop can perform a salt balance within soil profile, accounting for the salt derived from the water capillary rise and from the infiltration of saline irrigation water, and can calculate how much salt leaches out of the rooting zone. In particular, it simulates crop response to individual effects of salinity stress, as poor development of canopy cover and stomata closure, in terms of final biomass reduction.

AquaCrop has already been tested on different crops in multiple climatic and agro-ecological conditions. Given the relevance of maize as warm season irrigated crop in many world areas, only this crop is analysed here. Wang et al., (2015) adopted AquaCrop to investigate yield and water productivity for rainfed summer maize in the North China Plain. Salemi et al., (2011) and Oiganji et al., (2016) calibrated and validated the model for simulating maize growth under deficit irrigation in Northwest Iran and Northern Nigeria, respectively. Ahmadi et al., (2015), Kheir and Hassan (2016), Abedinpour et al., (2012), and Katerji et al., (2013) evaluated the effects of different irrigation techniques compared to rainfed regime, on maize yield in semi-arid areas of Iran, Egypt, Northern India, and Southern Italy, respectively. Only one study, however, was conducted on maize cultivated in saline environment (Saad et al., 2014).

This work addresses the calibration of the AquaCrop model for maize irrigation in the above referred coastal plain and its use to evaluate the effects of different irrigation strategies on salt accumulation. Several soil and plant parameters have been assessed during maize growth at field level and from remote sources, to assist in the calibration process. A first round of simulations is reported here and discussed to elucidate results already acquired, provide suggestions for irrigation strategy and highlight points needing additional effort. Section 2 describes the study area and its environmental conditions, the field surveys carried out to document phenological development and to validate and calibrate simulations. Section 3 describes survey results, the numerical model calibration, irrigation scenarios, model simulation results, and draws suggestions from simulations and observations for a proper irrigation scheduling. Section 4 presents a synthesis of major results.

2. Material and methods

2.1. The study area

The area surveyed within the Project is the coastal plain between the estuaries of Lamone (44°

31.661' N) and Reno (44° 35.432' N) rivers, around 7 km North of the port of Ravenna (Fig. 1). The area is comprised between the Adriatic coastline eastwards and the small town of S. Alberto (RA) westwards. The south-north road connecting today Ravenna to S. Alberto follows the coastal dune relief of the classic Etruscan period (500-300 b.C.); the entire study area is therefore part of the relatively recent deposits and is marked by intersecting ridges along the Etruscan, the medieval (followed by the Romea road connecting Venice to Rome), and the present littoral dunes, combined with riverine levee systems along the present Lamone, Destra Reno (ancient Lamone) and the present Reno (ancient Po di Primaro) river paths. The low lands between ridges were covered by brackish waters until the reclamation carried out in the last two centuries and finished in 1962. North of the Reno river and South of the present Lamone channel, coastal lagoons are still present (Lamberti et al., 2018). The agricultural study area, excluding dunes and levees, is therefore a low one with elevation ranging from -2 to +1 m a.s.l., and suffers from salt intrusion through the under-laying sandy aquifer. The area is artificially drained and can be irrigated with good quality water derived from the Reno river upstream the Voltascirocco barrage, as well as with low quality drainage water of the Destra Reno channel.

A field was selected (Fig.1) to test the model in the Biomarcabò unit of the Agrisfera Cooperative, which is involved as project partner.

2.2. Environmental conditions

The climate in the area is classified as Mediterranean North (Metzger et al., 2005), i.e. featuring a wet winter followed by a long growing season (7 months/yr, Apr. to Oct., of mean temperatures > 10 °C), but frequent and sometimes prolonged drought periods occurring in the summer time (July most critical), often requiring irrigation. The climate in the area features an average precipitation quite constant around the year (ca. 50 mm/month), whereas potential evapotranspiration is characterized by monthly values below 20 mm/month in Dec. and Jan., and a peak in July around 160 mm/month (Fig. 2).

Soil properties in the area are extremely variable, reflecting the different deposition processes. The field focused in this analysis is placed in the lowest part of the area that was seat for a lagoonal marsh in the 19th century; the soil texture is mainly silty-clayey or clayey. The readily available water (RAW) holding capacity of these soils is normally good, exceeding 100 mm, except for saline clays due to the high-water content at wilting point (WP).

Crops cultivated in the area are: winter cereals (wheat, barley) sown in October and harvested in June, the pluriannual forage lucerne, and summer crops as maize, sorghum, sunflower and soybean, sown in spring and harvested in the summer time. Only maize is regularly irrigated in the area.

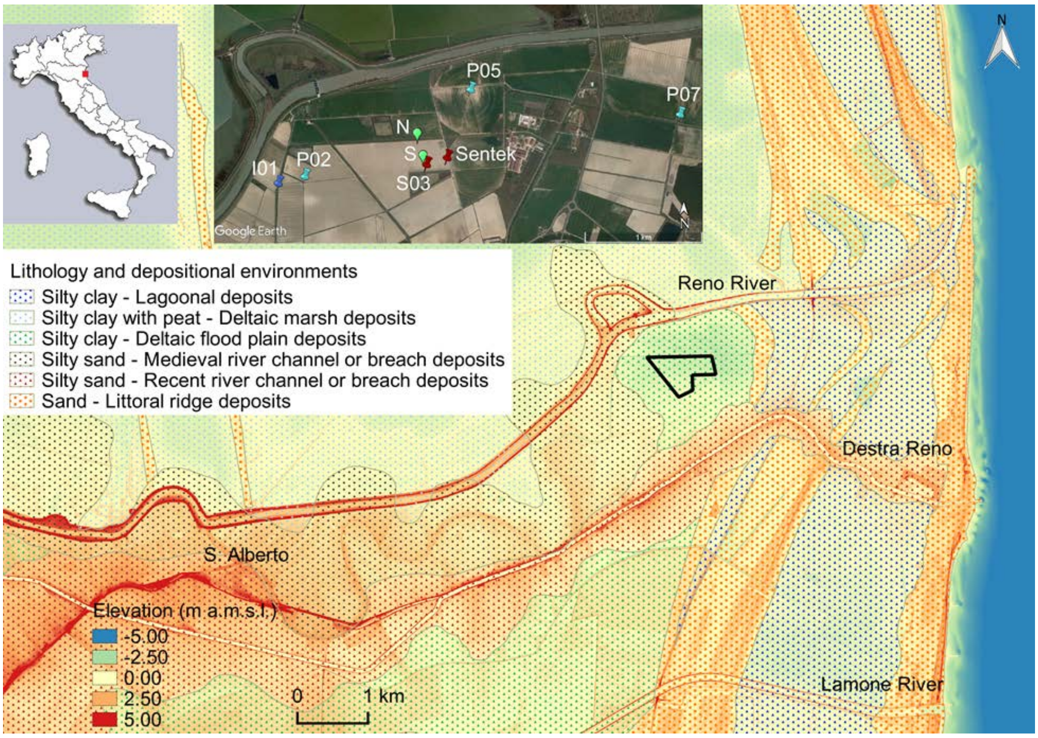

Fig. 1. The study area showing elevation, soil texture and depositional origin. The P02 and P07 marks indicate the meteorological stations provided with piezometers and soil sensors. The S03 and Sentek marks indicate the soil moisture and salinity sensors installed in the experimental field. The P05 mark indicates a further piezometer and soil sensor. N and S marks indicate the survey points in the field. The field involved in this paper is located in the lowest part of the area and its border is pointed out in Figure

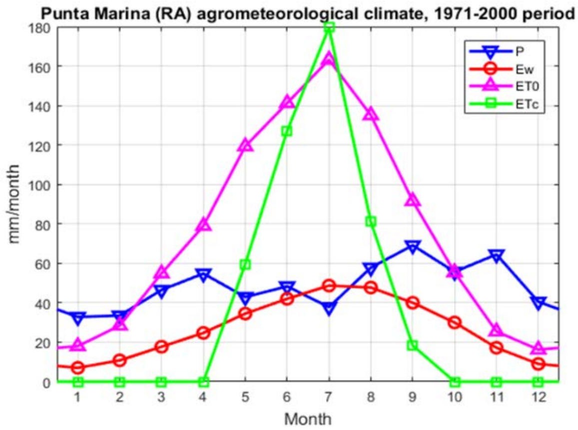

Fig. 2. Climatic conditions of the area

2.3. Groundwater and drainage

The area is artificially drained by two channel networks contained within major levees and ending with pumping stations pouring water into the Destra Reno channel, raising it from -3 m a.s.l to approximately the sea level. Agricultural fields were originally drained by ditches dug at a short spacing (around 25 m), reflecting the low permeability of soils. In order to increase the size of fields, in most part of the area ditches are now substituted by draining pipes, placed usually 90 cm below soil surface at 10 m spacing, with slope 1:1000 towards the drainage channel.

The drainage network depresses the water table well below sea level. Drainage pipes actually separate the upper agricultural soil, where water exceeding field capacity can percolate down draining salt and soluble nutrients, from lower layers, where saline or brackish water is normally present. In dry periods and non-irrigated fields, salt moves upwards by capillary rise and is concentrated at the soil surface in some areas.

Groundwater level and salinity were monitored in eight piezometers (denoted Pnn) of which three are visible in Fig. 1 (see also Cipolla et al., 2019); soil water content and bulk conductivity were monitored at 50 cm depth at piezometer stations and three further soil stations (e.g., S03 in Fig. 1). In the field object of this study, a temporary Sentek sensor measuring soil moisture and salinity down to 60 cm depth with 10 cm resolution was placed around start-up of the irrigation period to provide better information on water percolation in the soil (Fig. 3).

2.4. Maize cultivation

The experimental field was managed according to the principles of organic farming which are adopted in the specific unit of the Cooperative. The maize hybrid Krups (FAO 600), supplied by SIS (S. Lazzaro, Bologna, Italy), was sown on May 10, 2018, with a seed spacing of 15 cm on the row and 75 cm between rows. An average crop density of 7.8 plants m^{-2} was achieved after seedling emergence.

Soil was ploughed at 35 cm depth, harrowed and fertilized with the liquid fraction of digestate from cattle slurry before sowing. A second dose of liquid digestate was supplied during vegetative growth.

The crop was harvested on Aug 11, 2018, at the early dough stage. The whole plant was cut and chopped to produce maize silage.

The amount of water, supplied during maize growth by sprinkler irrigation operated with travelling gun, was determined by the farmer with the IRRINET software (http://www.consorziocer.it), a decision support system widely used in the area. This tool operating on an online platform calculates the real time water budget based on a crop growth model coupled with precipitation, the Hargreaves ET_0 (Hargreaves and Samani, 1985), and potentially the contribution of the shallow water table. Soil salinity is not accounted for.

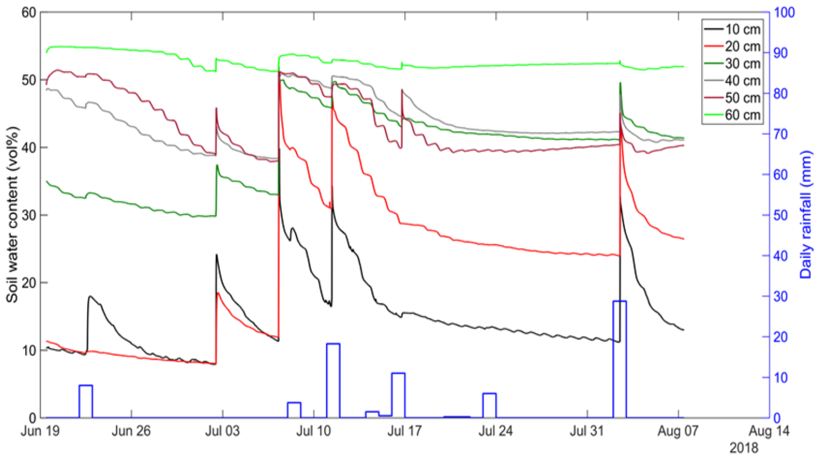

Fig. 3. Soil water content at different depths and rainfall recorded at stations Sentek and P02; with increasing depth average humidity as a consequence of rainfall or irrigation events normally increases while its time variation decreases; exceptions are present 1) due to cracks in the clayey soil, through which water can percolate to the deeper layers without increasing humidity of upper layers, and 2) superficial irrigation and rainfall in July are absorbed in the upper layers generating an inversion of the usual humidity gradient: in July humidity of the 40-50 cm deep layer is lower than in the 20-40 cm deep layers

2.5. Meteorological data

The climatic parameters fed to the AquaCrop model are: daily maximum and minimum air temperature (°C), relative humidity (%), average wind speed (km day^{-1}), precipitation (mm), global solar radiation (MJ m^{-2} day^{-1}) and average annual value of atmospheric CO_2 concentration. These data were derived from the measurements of the P02 meteorological station located near the field (Fig. 1). Missing data were replaced with data from the near P07 meteorological station.

The CO_2 concentration data, not recorded by the installed stations, were obtained from the Italian Air Force meteorological station (http://www.meteoam.it/pubpage/3/9) at Monte Cimone. A model integrated tool calculates the reference evapotranspiration ET_0 (mm day^{-1}) with the FAO Penman–Monteith equation (Allen et al., 1998).

2.6. Field surveys

Crop data. In order to verify information provided by the seed supplier, document crop development and check satellite information, a field survey of crop phenology, canopy development, root density distribution and biomass accumulation over time was carried out from May 9 to August 30 with weekly observations. Several crops were surveyed including maize in several fields. In the experimental field object of the present analysis, two monitoring points were established, one at the North and the other at the South side of the field (Fig. 1). Collected information include:

1. The principal maize growth stages were identified following the BBCH scale (Weber and Bleiholder, 1990; Lancashire et al., 1991) criteria. To achieve that, the plant height, number of leaves and nodes, start and end of the flowering period and fruit development were measured and recorded on a sample of 20 plants in each point. Average value was then calculated for each item.

2. Canopy Cover (CC, %) was derived from digital images produced by mobile devices in the field and subsequently processed using the Canopeo app for Matlab developed by Patrignani and Ochsner (2015). Ten photos were taken at each sampling point, five on the row and five on the inter-row. Average values were then calculated. Leaf area index (LAI) and Normalized Difference Vegetation index (NDVI) were also assessed, the first by sampling five random plants and measuring leave surface, the second systematically using the instrument GreenSeeker (Trimble Ag Field Solutions, Sunnyvale, CA, USA).

3. Plant biomass was measured with a 3-week interval, starting from the stem elongation phase. The plants on two adjacent rows per 2 m length were cut from the base and weighed with a dynamometer to determine the fresh weight (kg m^{-2}). A sub-sample was oven-dried at 105°C to determine the dry weight (kg m^{-2}).

4. Root density was measured at flowering end, when root growth is considered completed. Root samples were taken by coring the soil with a one-meter deep steel cylinder, 8 cm in diameter. The extracted soil column was divided in 20 cm long portions. Soil was washed-out and the remaining roots were weighed with a precision scale. Root volume density was calculated according with Wu et al., (2017).

5. The field received a total 135 mm irrigation in three interventions (June 20, July 10 and 19; exact dates slightly vary due to sprinkler displacement to cover the large field).

2.7. Model criteria

AquaCrop model version 6 was used. It was tested first by comparison with observed data, and then used to simulate irrigation management scenarios. For model calibration the following data were used.

a. Crop data. The crop module was implemented in Growing Degree Days (GDD). The default values provided by the FAO AquaCrop model for the maize crop parameters were modified according to the specific characteristics of the hybrid used. The GDD data provided by the seed supplier were used for this purpose. FAO default stress-coefficients were left unchanged.

b. Field management. Soil fertility and weed management were set as optimal in the model. The soil Curve Number (CN) based on soil textural class was reduced by 5% to account for soil tillage effect on soil permeability and water infiltration rate.

c. Soil characteristics. Soil moisture and salinity were monitored throughout the crop growing season using two sensors (GS3-Meter and Sentek) located at the South and East side of the field (Fig. 1). Four soil layers of variable depth were considered in the model: 0-10, 10-30, 30-60, 60-120 cm depth (Table 1). Soil hydraulic properties, water content at saturation (SAT), field capacity (FC), permanent wilting point (PWP) and saturated hydraulic conductivity (K_{sat}), were calculated by means of the Soil Water Characteristic software (Saxton and Rawls, 2006) based on soil texture, compaction, organic matter and salinity. Calculated parameters were further adjusted based on the Sentek moisture readings at 10 cm depth intervals, to better represent tillage driven porosity variation along depth and its influence on water infiltration and holding capacity.

d. Groundwater. Groundwater level and salinity were monitored by means of the P02 and P05 piezometers installed in the pilot area close to the experimental field (Fig. 1). Groundwater level and salinity observed at P02 were therefore imposed to this module. Starting from June 19, the above described network of plastic pipes located below field surface was flooded with fresh water by raising water level in the discharging ditch at the north boundary of the field; however, the fresh water lens due to pipe slope did not extend to the whole field, but only to around half the field, i.e. the northern part near the ditch. Owing to this, the following two conditions were represented in simulations as groundwater boundary conditions:

- P02 observed groundwater level and salinity (brackish groundwater, BG);
- constant fresh water lens of good quality at 80 cm depth (flooded drains, FD).

e. Initial conditions. The simulation was run starting on April 1st using: 1) for water content and salinity of the 3rd layer, values obtained from records of the GS03 sensor installed in the field, and 2) a regular gradient of water content and salinity along the vertical. The 40-day long simulation before actual sowing (May 10) reduces the effect of the initial gradient once the relevant simulation phase starts.

f. Irrigation. Irrigation water quality was set as good, according to the results of the monitoring done during the growing season. The real irrigation events are reproduced in the calibration phase.

3. Results and discussion

3.1. Crop development

The development of the crop followed almost exactly the anticipated schedule based on the pattern indicated by the seed supplier. Ground observed CC and NDVI values matched quite well values obtained from Sentinel 2 and Landsat 8 satellite observations, respectively with 10 and 30 m resolution. Until flowering, NDVI and CC showed practically equal numerical values, whereas after flowering both remained almost constant and therefore could not describe the final reproductive and crop ripening phase.

Fig. 4 presents NDVI values at the two survey points in the field. Growth in space and time was fairly consistent; the spatial distribution at the end of the vegetative stage can be observed from the NDVI satellite image at June 30 (just before flowering) presented in Fig. 5a.

As a partial conclusion, the space-time pattern of the crop vegetative development is coherently described by ground and satellite observations of the NDVI parameter.

3.2. Final crop yield

At harvesting time, a big cutter-shredder machine was used equipped with a crop mass and humidity measuring system and GPS positioning, so that the detailed yield map for the field was produced that is shown in Fig. 5b. Point measurements and the continuous map obtained by kriging are shown in the Figure.

Table 1. Physical and hydraulic properties at increasing soil depths at the Biomarcabò field

Horizon	*Depth (cm)*	*Textural Class*	*SAT (% vol)*	*FC (% vol)*	*PWP (% vol)*	*K_{sat} (mm·day^{-1})*	*Compaction*
1	0-10	Silty clay	58.5	41.5	27.0	283	loose
2	10-30	Silty clay	58.5	41.5	27.0	283	loose
3	30-60	Silty clay	53.9	40.6	26.9	138	normal
4	60-120	Silty clay	47.0	39.2	26.8	31	dense-hard

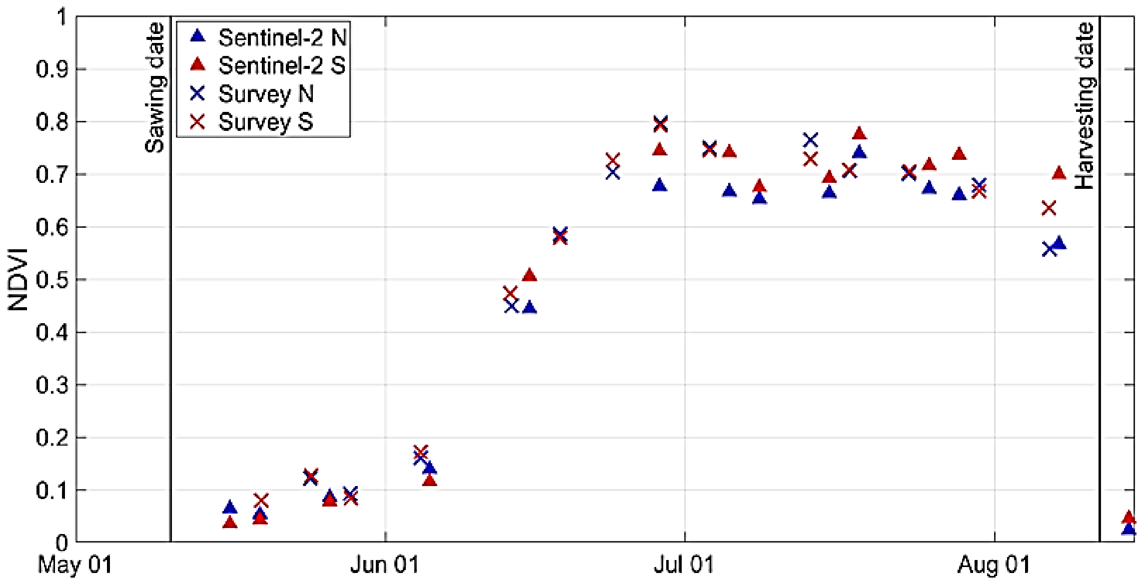

Fig. 4. Time evolution of NDVI at the survey points according to different sources: ground observations at positions N/S, and Sentinel 2 observations at the same positions, obtained from the EO Data Service (http://www.eodataservice.org/).

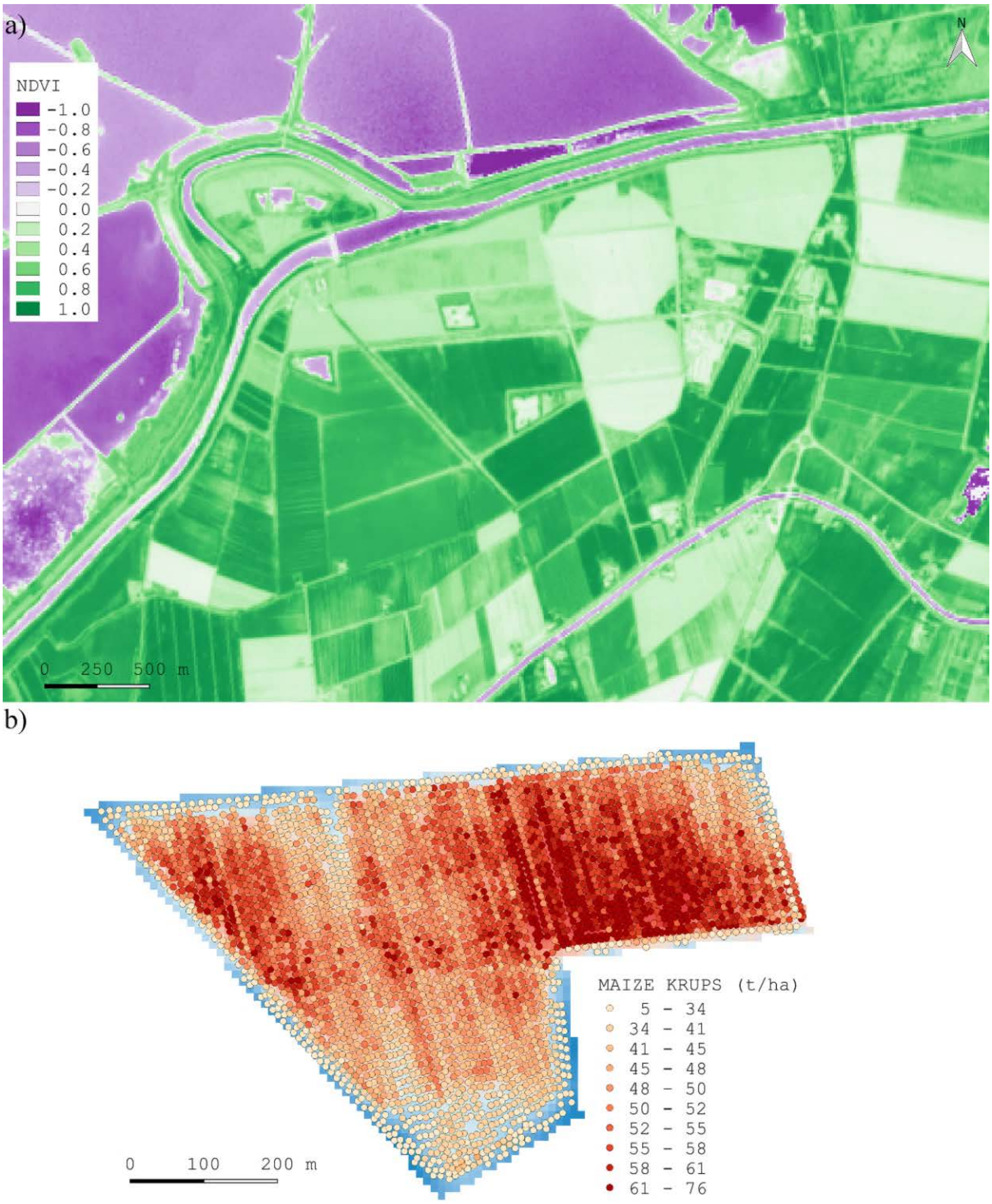

Fig. 5. NDVI distribution over the area on June 30, 2018, i.e. after the first irrigation and just before flowering-a). Yield map at harvesting time in the surveyed field -b)

Some features of maps in Fig. 5 are common, and in fact their correlation coefficient is high (0.80), showing that most processes that limit yield in the field are not varying in time and are presumably related to soil conditions.

3.3. Model calibration

The agreement between model results and field observations was already good with the standard parameters. Only a minor adjustment to initial leaf area was necessary to catch the initial growth speed of the crop. Fig. 6a reports the results of a preliminary simulation in the calibration phase. Based on field observations, the calibrated parameters initial leaf area and initial root depth were finally assumed equal to 8 cm^2/plant and 25 cm. Model results can be compared with observations as far as canopy cover and dry crop mass per unit surface are concerned; Fig. 6b shows the excellent results obtained.

The model, therefore, can be considered successfully calibrated, so that reliable conclusions can be drawn from the simulation of different irrigation strategies.

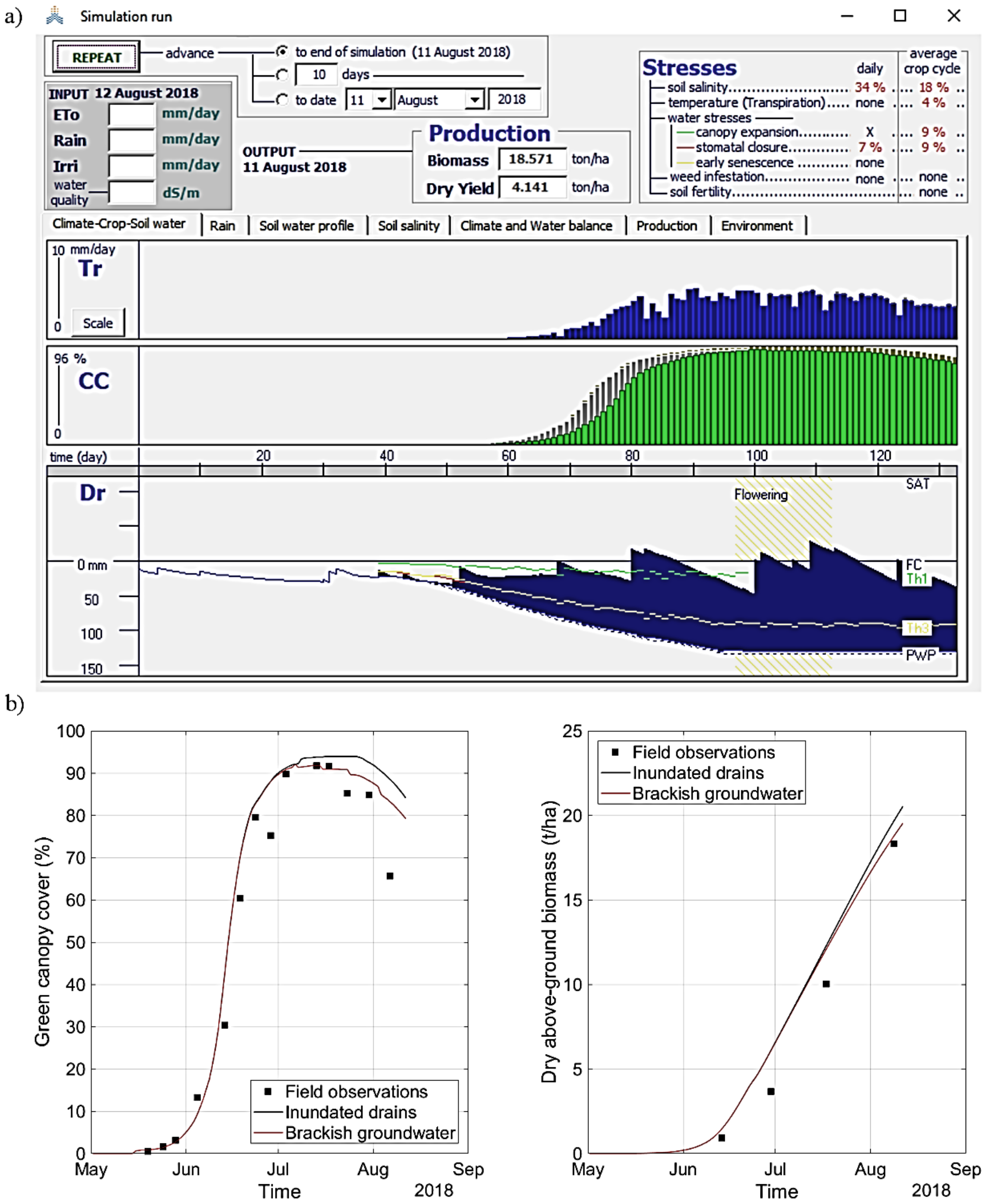

Fig. 6. Time evolution of soil water content during a preliminary simulation in calibration phase, with the standard initial leaf area of 6.50 cm^2/plant and 15 cm initial root depth, AquaCrop graphical output; the combination of a rather dry May with the adopted parameters results in a delayed simulated crop development (the green CC graph) compared to the optimal one (the grey one)-a). Comparison between final calibrated model results and field observations at survey point N (Fig. 1) for the two parameters that are simulated and observed-b)

3.4. Implemented irrigation criteria

The irrigation module was set on "generation of an irrigation schedule" mode, and the sprinkler irrigation method, wetting 100% of the soil surface, was selected. The model was asked to establish an irrigation event whenever the Readily Available Water (RAW) was depleted below a given level M_{min} while the irrigation volume is set indirectly fixing an upper level M_{max} to be reached, which is not far from field capacity. The two levels may vary in time to follow crop sensitivity to water stress during its development. Due to practical reasons and following regional suggestions, that aim at preserving the water resource, a maximum 50 mm per irrigation event is normally proposed. Since this amount is significantly lower than RAW in soils of the area, irrigation may be scheduled keeping soil humidity around the lower RAW limit in order to reduce leaching due to unforeseen rainfall events, or around the upper limit aiming to produce some leaching; the following criteria are in fact tested.

The 1st criterion is similar to the standard suggested for Maize (http://www.fao.org/land-water/databases-and-software/crop-information/maize/en/) by FAO Land & Water: "to obtain a good stand and rapid root development the root zone should be wetted at or soon after sowing"; the acceptable water depletion level is about 40% in the establishment period, between 55 and 65% during the vegetative, flowering and yield formation periods, and 80% during the ripening period. Here and in what follows, percent figures refer always to RAW depletion level, as used in AquaCrop.

In the surveyed Region, irrigation is usually discouraged until June since in April and May soil water content accumulated in winter time is usually sufficient; therefore a 2nd criterion is simulated representing the local irrigation strategy. Irrigation is proscribed until June; M_{min} is then set at 80% of RAW depletion; starting from stem elongation, M_{min} is gradually raised to reach 65% at flowering start, when the maize plants are most sensitive to water stress. From the flowering end, M_{min} is gradually lowered attaining the initial 80% at the end of the ripening phase, i.e. at the dough stage, and irrigation is inhibited in August, since harvesting in the given circumstances (sowing date, seed hybrid and accumulated GDD) is scheduled no later than August 15. Irrigation depth is fixed at 50 mm (M_{max} adapted to obtain this depth). This criterion results in a rather water conservative one, based on most common conditions in the region.

In the 3rd criterion, M_{min} is kept constant at 50% of RAW and irrigation volume fixed as the amount restoring water content at field capacity (M_{max}). This criterion aims at maintaining yield potential at the expense of some inefficient water utilisation when a heavy rainfall occurs just after an irrigation event; in any case, since FC is not intentionally exceeded, leaching is not intentionally produced.

Since none of the previous criteria represents an intentional leaching strategy, a further criterion, the 4th, is simulated where M_{min} is fixed at 40% and irrigation amount is controlled to produce a 5 mm excess above FC. Finally, since several of the previous irrigation criteria cause a number of irrigation events greater than usual and might result non sustainable from an economic point of view, a 5th scenario is introduced where irrigation is inhibited in May and August, the lower and upper levels for irrigation are set at 50% of RAW and FC+10 mm respectively.

Actual irrigation and the 2nd criterion result in salinization prone strategies, whereas all the others criteria aim at controlling salt accumulation in soil. All irrigation criteria are simulated under BG conditions as well as under FD conditions. The main results obtained by AquaCrop (Fig. 7 refers for example to the 1st criterion with brackish groundwater) are presented in Table 2.

Table 2. Synthesis of results of the tested scenarios for the simulation period April 1 – August 11, 2018.

Irrigation criterion	***Crop yield, dry above-ground biomass (t/ha)***	***Irrigation depth (mm) and events***	***Final salt content in the root zone (t/ha)***	***Crop transpiration (mm)***	***Runoff (mm)***
2018, FD	20.524 (94%)	135 (3)	8.436	266.4	6.7
2018, BG	19.524 (90%)	135 (3)	17.404	253.4	6.3
1, FD	21.050 (97%)	134.7 (4)	8.440	273.1	4.0
1, BG	20.032 (92%)	123.8 (3)	17.398	259.9	7.0
2, FD	20.508 (94%)	147.8 (4)	8.411	266.2	4.1
2, BG	19.513 (90%)	135.2 (3)	17.400	253.3	7.3
3, FD	21.053 (97%)	152.7 (4)	8.540	273.1	2.4
3, BG	20.029 (92%)	168.3 (4)	17.550	259.9	4.6
4, FD	21.061 (97%)	184.4 (5)	8.680	273.2	7.0
4, BG	20.025 (92%)	154.9 (4)	17.506	259.8	2.5
5, FD	20.524 (94%)	155.5 (3)	8.501	266.4	2.9
5, BG	19.524 (90%)	105.7 (2)	17.348	253.4	3.1
5, FD since 11/5	21.179 (97%)	154.1 (3)	7.620	274.9	2.6

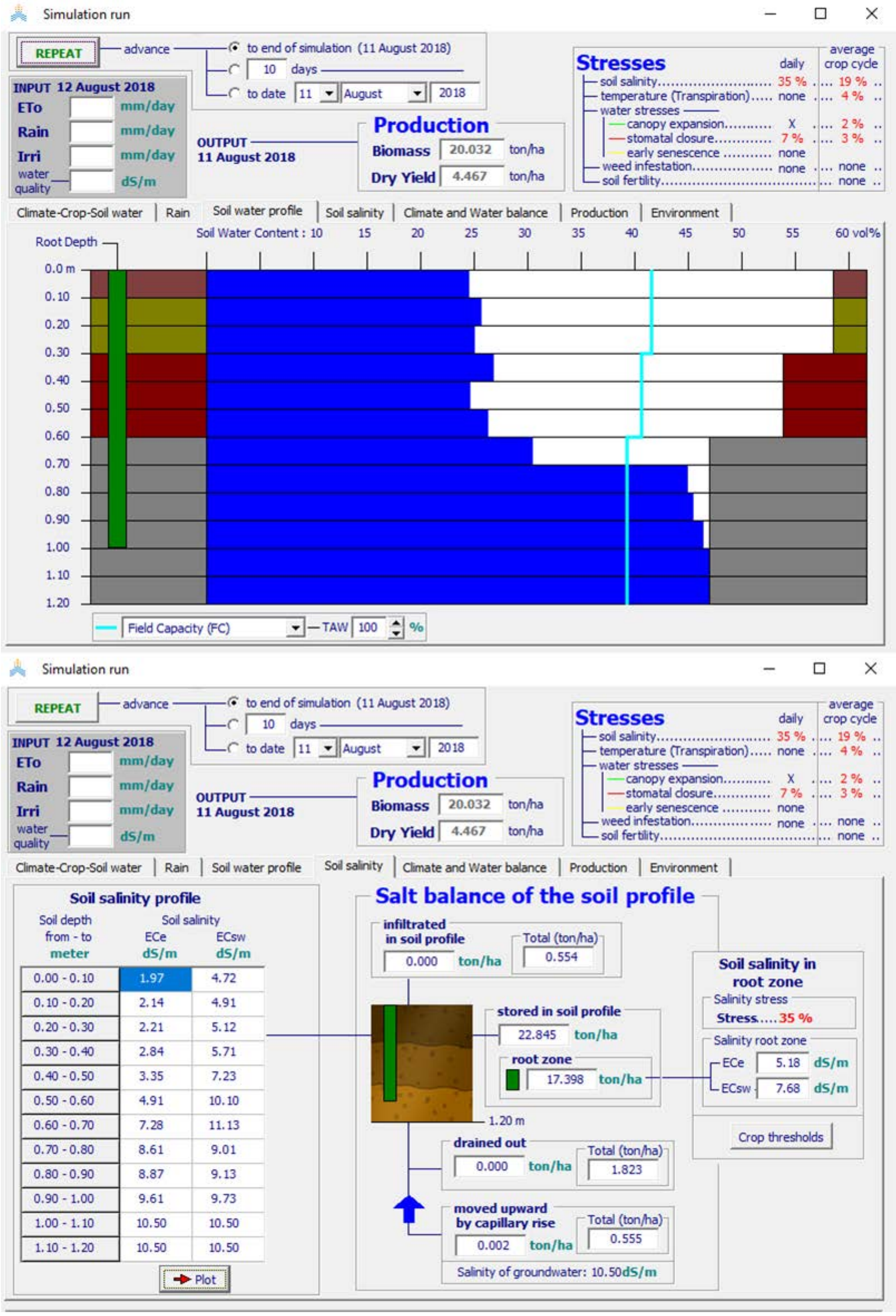

Fig. 7. Vertical distribution of water and salt content in the soil at harvesting time for scenario 1 with brackish groundwater, AquaCrop graphical output.

Crop yield, i.e. dry above-ground biomass, is presented also as percentage of the potential yield under no stress conditions (21.763 t/ha). The salt content at sowing time within the final root depth is around 9.0 t/ha; therefore, all the FD scenarios represent a moderate reduction of salt content in soil, whereas all BG scenarios represent a significant increase of soil salt content.

3.5. Effects of irrigation strategy on crop yield and soil salinization

It must be focused that the 2018 summer season was not an arid one: 190.1 mm rainfall occurred in the simulation period, most of which in June and July. Irrigation criteria are all based on the current soil water content and no rainfall forecast is accounted for. Therefore, when simulation results are analysed the reader must be aware of 1) the weak relevance of irrigation in the period, and 2) the uncontrolled occurrence of rainfall after irrigation events, a circumstance that introduces some random behaviour, obscuring the systematic average effect of the criterion.

In any case, a major systematic effect is due to inundated drains. It decreases significantly the accumulation of salt in the agricultural soil originating from groundwater by capillary rise under a water content gradient, and the consequent salinity stress. Crop yield and transpiration are increased, and this forced sometimes an additional irrigation event (40-50 mm) by the end of July, producing a weak benefit since a significant rainfall event occurred at the beginning of August.

The best results, both for crop yield and salinization control, were obtained by inundating drains just after sowing. The depth-time evolution of soil water and salinity content during the growing season is presented in Fig. 8. The general behaviour of salinization prone scenarios is represented in Fig. 8a-b, where salt rising is apparent in absence of flooded drains. All the other scenarios are qualitatively represented in Fig. 8c-d, where the earliest drain inundation scenario (5^{th} - FD since 11/5) and one of the most water consuming scenarios (3^{rd} - BG) over brackish groundwater are represented.

The former is able to contrast salt rising-up, whereas the latter does not involve a sufficient amount of irrigation water to produce a complete soil leaching; percolation is limited to the first superficial layers and salt is not removed from the whole soil column.

3.6. Discussion and suggestions for irrigation scheduling

In the absence of inundated drains, the agricultural soil is dried up in late spring and summer and salt rises regularly towards the surface. In summertime, irrigation and rainfall events do not usually compensate the prevailing transpiration, but cause fluctuations of water content in the shallow layers. This is what was observed by the Sentek sensor, placed in the upper part of the field beyond the limits of inundated drains action. When and where drains are inundated (in 2018 drains were inundated at the first irrigation time), capillary rise, that is particularly active where humidity gradient is intense, draws fresh water up, whereas brackish water is not subject to relevant humidity gradient and does not rise. If drains are inundated before the formation of the drying front in the soil, i.e. in May, salt accumulation in soil is almost completely avoided.

The irrigation practice in the area and the regional government suggestions are conditioned by experience in the prevalent environmental conditions, where groundwater is several meters below the soil surface and soil surface has a non-vanishing slope. Therefore, water percolating from the top soil is assumed to be lost for agriculture and irrigation is not practiced by flooding that involves low energy consumption (less than 1 m head drop), need of manpower and water use efficiency (50%), but mainly with sprinkler that requires energy (several 10 m head) and significant amount of manpower to obtain a high water use efficiency.

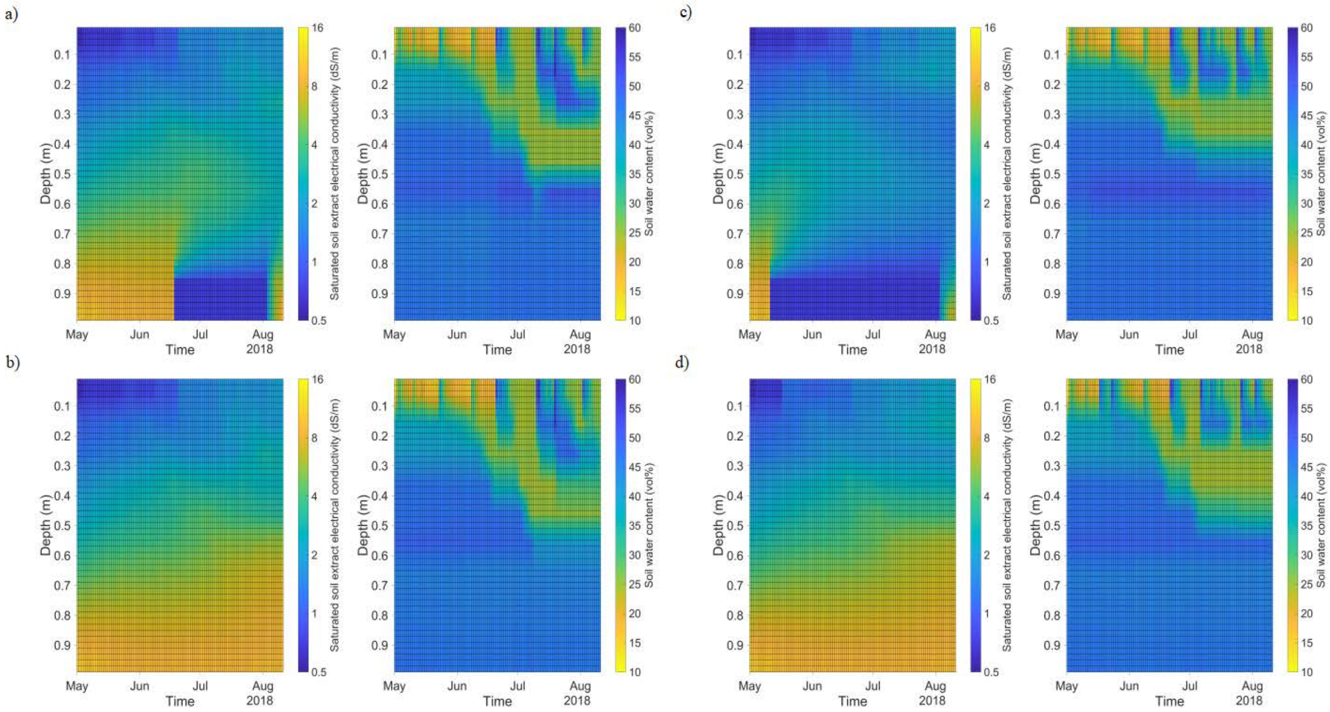

Fig. 8. Depth-time distribution of salinity and water content in the case of inundated drains (a) and brackish groundwater (b) considering the actual 2018 irrigation scenario. Depth-time distribution of salinity and water content in the case of irrigation scenario 5 with inundated drains just after sowing (c) and irrigation scenario 3 with brackish groundwater (d)

This water saving strategy is not justified in the lowest areas of the basin, where water flowing in rivers if not used is poured into the sea, or if flowing in the drainage channels and not used must be pumped up to the sea level.

Drainage pipes are very useful to keep the soil dry without sub-dividing large agricultural areas in many small fields divided by ditches, but can also be profitably used for subsoil irrigation preventing salt rising from brackish groundwater. Some minor adaptation can be suggested for the double use as reducing the slope (from 1 m/km to 0.5 m/km) and/or placing pipes with a double slope from the field centre to the surrounding ditches, so that with 0.1 m submergence at drain outlet the served length of the field may increase from 100 m to 200 or 400 m.

4. Conclusions

Field survey and satellite images provide an adequate description of crop growth and development.

AquaCrop is a reliable model to anticipate crop development and yield also in areas exposed to salinization, as well as to simulate effects of irrigation strategy on salt accumulation in soils.

Subsoil pipe drainage was introduced in the area to extend field surfaces and use large capacity field equipment; it has shown to be also an efficient tool to contrast soil salinization where a humid season, as winter is in the study area, causes some natural leaching.

The utilization of subsoil drains for irrigation generates a fresh water lens quite effective as a barrier against capillary rise of brackish water and salt accumulation in the agricultural soil.

The survey year (2018) was not an arid one, therefore crop yield and irrigation resulted weakly sensitive to the adopted irrigation strategy.

All the tested leaching strategies were not completely effective in the simulated period (spring and summer), and presumably need a humid climate for the remaining seasons to remove salt in a year cycle.

The irrigation practice most diffused in the Emilia-Romagna region is probably not appropriate for the lowest areas near the sea, where reducing the consumption of fresh flowing water, when available, is nonsense.

Acknowledgements

The work has been financed by the LIFE 2014-2020 Programme, through the LIFE AGROWETLANDS II - Smart Water and Soil Salinity Management in Agro-Wetlands (LIFE15 ENV/IT/000423) Project.

References

Abedinpour M., Sarangi A., Rajput T.B.S., Singh M., Pathak H., Ahmad T., (2012), Performance evaluation of AquaCrop model for maize crop in a semi-arid environment, *Agricultural Water Management*, **110**, 55-66.

Abrol I.P., Yadav J.S.P., Massoud F.I., (1988), *Salt-Affected Soils and Their Management*, FAO, Rome, Italy.

Ahmadi S.H., Mosallaeepour E., Kamgar-Haghighi A.A., Sepaskhah A.R., (2015), Modeling maize yield and soil water content with AquaCrop under full and deficit irrigation managements, *Water Resources Management*, **29**, 2837-2853.

Allen R.G., Pereira L.S., Raes D., Smith M., (1998), *Crop Evapotranspiration – Guidelines for Computing Crop Water Requirements*, FAO, Rome, Italy.

Antonellini M., Mollema P., Giambastiani B., Bishop K., Caruso L., Minchio A., Pellegrini L., Sabia M., Ulazzi E., Gabbianelli G., (2008), Salt water intrusion in the coastal aquifer of the southern Po Plain, Italy, *Hydrogeology Journal*, **16**, 1541-1556.

Buscaroli A., Zannoni D., (2010), Influence of ground water on soil salinity in the San Vitale Pinewood (Ravenna - Italy), *Agrochimica*, **LIV**, 303-320.

Cipolla S.S., Maglionico M., Masina M., Lamberti A., Daprà I., (2019), Real time monitoring of water quality in an agricultural area with salinity problems, *Environmental Engineering and Management Journal*, **18**, 2229-2240.

Crescimanno G., Iovino M., Provenzano G., (1995), Influence of salinity and sodicity on soil structural and hydraulic characteristics, *Soil Science Society of America Journal*, **59**, 1701-1708.

Felisa G., Ciriello V., Di Federico V., (2013), Saltwater intrusion in coastal aquifers: A primary case study along the Adriatic coast investigated within a probabilistic framework, *Water*, **5**, 1830-1847.

Greggio N., Mollema P., Antonellini M., Gabbianelli G., (2012), *Irrigation Management in Coastal Zones to Prevent Soil and Groundwater Salinization*, In: *Resource Management for Sustainable Agriculture*, Abrol V., Sharma P. (Eds.), IntechOpen.

Hargreaves G.H., Samani Z.A., (1985), Reference crop evapotranspiration from temperature, *Applied Engineering in Agriculture*, **1**, 96-99.

Jones J.W., Hoogenboom G., Porter C.H., Boote K.J., Batchelor W.D., Hunt L.A., Wilkens P.W., Singh U., Gijsman A.J., Ritchie J.T., (2003), The DSSAT cropping system model, *European Journal of Agronomy*, **18**, 235-265.

Katerji N., Campi P., Mastrorilli M., (2013), Productivity, evapotranspiration, and water use efficiency of corn and tomato crops simulated by AquaCrop under contrasting water stress conditions in the Mediterranean region, *Agricultural Water Management*, **130**, 14-26.

Keating B.A., Carberry P.S., Hammer G.L., Probert M.E., Robertson M.J., Holzworth D., Huth N.I., Hargreaves J.N.G., Meinke H., Hochman Z., McLean G., Verburg K., Snow V., Dimes J.P., Silburn M., Wang E., Brown S., Bristow K.L., Asseng S., Chapman S., McCown R.L., Freebairn D.M., Smith C.J., (2003), An overview of APSIM, a model designed for farming systems simulation, *European Journal of Agronomy*, **18**, 267-288.

Kheir A.M.S., Hassan, M.A.A., (2016), Performance assessment of the FAO Aquacrop model for maize yield, biomass and water productivity along the River Nile, Egypt, *Journal of Soil Sciences and Agricultural Engineering, Mansoura University*, **7**, 721-728.

Lamberti A., Masina M., Lambertini A., Borgatti L., (2018), *Salt Contamination in the Coastal Zone between Reno and Lamone Rivers: Influence of Geomorphic Conditions on Sea Water Intrusion*, Proc. XXXVI Italian Conf. on "Water Engineering", Ancona, Italy, On line at: https://www.dropbox.com/sh/yxoqmddkv0k1w6e/AABQesECcU3e9QucwkxEf2oHa?dl=0,Memorie/paper_317.

Lancashire P.D., Bleiholder H., Van den Boom T., Langelüddeke P., Stauss R., Elfriede Weber, Witzenberger A., (1991), A uniform decimal code for growth stages of crops and weeds, *Annals of Applied Biology*, **119**, 561-601.

Metzger M.J., Bunce R.G.H., Jongman R.H.G., Mücher C.A., Watkins J.W., (2005), A climatic stratification of the environment of Europe, *Global Ecology and Biogeography*, **14**, 549-563.

Oiganji E., Igbadun H.E., Mudiare O.J., Oyebode M.A., (2016), Calibrating and validating AquaCrop model for maize crop in Northern zone of Nigeria, *Agricultural Engineering International: CIGR Journal*, **18**, 1-13.

Patrignani A., Ochsner T.E., (2015), Canopeo: A powerful new tool for measuring fractional green canopy cover, *Agronomy Journal*, **107**, 2312-2320.

Saad A.M., Mohamed M.G., El-Sanat G.A., (2014), Evaluating AquaCrop model to improve crop water productivity at North Delta soils, Egypt, *Advances in Applied Science Research*, **5**, 293-304.

Salemi H., Soom M.A.M., Lee T.S., Yusoff M.K., Ahmad D., (2011), Effects of deficit irrigation on water productivity and maize yields in arid regions of Iran, *Pertanika Journal of Tropical Agricultural Science*, **34**, 207-216.

Saxton K.E., Rawls, W.J., (2006), Soil Water Characteristic Estimates by Texture and Organic Matter for Hydrologic Solutions, *Soil Science Society of America Journal*, **70**, 1569-1578.

Shainberg I., Levy G.J., Rengasamy P., Frenkel H., (1992), Aggregate stability and seal formation as affected by drops' impact energy and soil amendments, *Soil Science*, **154**, 113-119.

Steduto P., Hsiao T.C., Raes D., Fereres E., (2009), AquaCrop—The FAO crop model to simulate yield response to water: I. Concepts and underlying principles, *Agronomy Journal*, **101**, 426-437.

Stöckle C.O., Donatelli M., Nelson R., (2003), CropSyst, a cropping systems simulation model, *European Journal of Agronomy*, **18**, 289-307.

Teatini P., Ferronato M., Gambolati G., Gonella M., (2006), Groundwater pumping and land subsidence in the Emilia-Romagna coastland, Italy: Modeling the past occurrence and the future trend, *Water Resources Research*, **42**, W01406.

Tóth G., Adhikari K., Várallyay Gy., Tóth T., Bódis K., Stolbovoy V., (2008), *Updated map of salt affected soils in the European Union*, In: *Threats to Soil Quality in Europe*, Tóth G., Montanarella L., Rusco E. (Eds.), Office for Official Publications of the European Communities, Luxembourg, 65-77.

Tsanis I.K., Daliakopoulos I.N., Koutroulis A.G., Karatzas G.P., Varouchakis E., Kourgialas N., (2016), *Soil Salinization*, In: *Soil Threats in Europe: Status, Methods, Drivers and Effects on Ecosystem Services*, Stolte J., Tesfai M., Øygarden L., Kværnø S., Keizer J., Verheijen F., Panagos P., Ballabio C., Hessel R. (Eds.), 104-116.

Vanuytrecht E., Raes D., Steduto P., Hsiao T.C., Fereres E., Heng L.K., Garcia Vila M., Mejias Moreno P., (2014), AquaCrop: FAO's crop water productivity and yield response model, *Environmental Modelling & Software*, **62**, 351-360.

Visconti F., De Paz J.M., Rubio J.L., Sánchez J., (2011), SALTIRSOIL: a simulation model for the mid to long-term prediction of soil salinity in irrigated agriculture, *Soil Use and Management*, **27**, 523-537.

Wang J., Huang F., Li B., (2015), Quantitative analysis of yield and soil water balance for summer maize on the piedmont of the North China Plain using AquaCrop, *Frontiers of Agricultural Science and Engineering*, **2**, 295-310.

Weber E., Bleiholder H., (1990), Explanations of the BBCH decimal codes for the growth stages of maize, rape, faba beans, sunflowers and peas - with illustrations, (Erläuterungen zu den BBCH-Dezimal-Codes für die Entwicklungsstadien von Mais, Raps, Faba-Bohne, Sonnenblume und Erbse - mit Abbildungen), *Gesunde Pflanzen*, **42**, 308-321.

Wu Y., Wang H., Yang X., Meng Z., He D., (2017), Soil water effect on root activity, root weight density, and grain yield in winter wheat, *Crop Science*, **57**, 437-443.

Yang H.S., Dobermann A., Lindquist J.L., Walters D.T., Arkebauer T.J., Cassman K.G., (2004), Hybrid-maize–a maize simulation model that combines two crop modeling approaches, *Field Crops Research*, **87**, 131-154.